Published in final edited form as:
Am J Physiol Heart Circ Physiol. 2008 June ; 294(6): H2898–H2904. doi:10.1152/ajpheart.91488.2007.

Incidence of protein on actin bridges between endothelium and smooth muscle in mouse arterioles demonstrates heterogeneous connexin expression and phosphorylation

Brant E. Isakson[1,2,*], **Angela Best**[2], and **Brian R. Duling**[1,2]

[1] Department of Molecular Physiology and Biological Physics, University of Virginia Health Science System, P.O. Box 801394, Charlottesville, VA 22908

[2] Robert M. Berne Cardiovascular Research Center, University of Virginia Health Science System, P.O. Box 801394, Charlottesville, VA 22908

Abstract

Although much physiology in resistance vessels has been attributed to cytoplasmic connection between endothelial cells (EC) and vascular smooth muscle cells (VSMC), little is known of protein expression between the two cell types. In an attempt to identify proteins between EC and VSMC, mouse cremaster arterioles were stained with phalloidin-Alexa594 and viewed on a confocal microscope which resolved “actin bridges” within the internal elastic lamina between EC and VSMC. To determine the incidence of protein, the pixel intensity from the antibodies on actin bridges were compared to the pixel intensity from antibodies within EC or VSMC. N-cadherin, desmin, connexin (Cx)40 and Cx43 and phosphorylated Cx43 at serine 368 were identified on actin bridges but NG2, CD31 and Cx45 were not evident. Connexin37 expression was more variable than the other connexins examined. Using this method on rat mesentery, we confirm the previously published predominance of Cx37 and Cx40 at the myoendothelial junction that was determined using electron microscopy. We conclude that this new method represents an important screening mechanism in which to rapidly test for protein expression between EC and VSMC, and possibly a first-step in quantifying protein expression at the myoendothelial junction.

Keywords

myoendothelial junctions; connexin; phosphorylation; N-cadherin

Introduction

Within resistance vessels, immunocytochemistry has demonstrated the presence of multiple connexin isoforms within endothelial cells (EC; e.g., (15;17)) and vascular smooth muscle cells (VSMC; e.g., (15;23)). However, analysis of the incidence of protein expression between EC and VSMC from resistance vessels has not been done. This is vital to understanding EC and VSMC integration as it reveals possible differences in how the two cell types may utilize connexins for heterocellular communication (e.g., (2)).

One of the most anatomically unique areas of resistance vessels is the location between EC and VSMC, where the two cell types make physical contact, termed the myoendothelial junction (MEJ). The MEJ is formed when EC and/or VSMC extend cellular extensions

* to whom correspondence should be addressed: P: 434-409-9397, F: 434-924-6899, E: bei6n@virginia.edu.

through the internal elastic lamina (IEL) and make contact. Since Rhodin identified MEJs in transmission electron microscopy (TEM) sections of arterioles, it has been suggested that the MEJ acts as a possible “nexus” of signaling molecules and receptors between arteriolar EC and VSMC (20). However, the size of the MEJ (approximately 0.5 μm by 0.5 μm width and length) and its location between EC and VSMC, has made assessment of protein expression such as connexins, dependent on TEM (23) or resorting to a cell-culture based model (6). Because of this, little is known of the MEJ in terms of protein expression; structurally however, we do know that it can contain endoplasmic reticulum (7), and because MEJs are cellular extensions, must be membranous and contain actin.

It has been hypothesized that gap junctions play a key role in integration of VSMC and EC function (e.g., (18)). Using TEM, previous work has confirmed that the typical gap junctional “pentalaminar” structure is present between EC and VSMC at the MEJ in resistance vessels (22;29). Connexin proteins compose gap junctions by forming a dodecameric channel linking two adjacent cells. The gap junction channel permits cell-cell communication either on a rapid (e.g., second messengers and current flow) or a slower (e.g., control of mitosis) time scale, with recent work demonstrating roles in intracellular communication (32). Because the types of connexin isoforms determines solute permeability (e.g., (16)), and thus cellular responses, providing information as to the degree and type of heterogeneous connexin expression between EC and VSMC would provide powerful insight into how EC and VSMC are functionally integrated.

Here we present a method whereby protein expression, as detected by antibodies, can be evaluated between EC and VSMC. This method utilizes phalloidin labeled with a fluorescent conjugate to track actin-based cellular extensions through the IEL, identified using Z-sections produced by confocal microscopy. By overlaying the “actin-bridges” in the IEL and connexin antibodies as revealed with a fluorescent tag, we plot the incidence of connexin proteins found in the cellular extensions linking EC and VSMC in mouse arterioles, and compare it to rat mesenteric arteries where connexin detection at the MEJ has utilized electron microscopy. We believe this method will enable rapid screening for protein between EC and VSMC, and is an important first-step towards quantification of protein at the MEJ.

Materials and Methods

Animals

All C57/Bl6 mice (Taconic) were males between 6–10 weeks of age and were use according to the University of Virginia Animal Care and Use Committee guidelines. Mice were euthanized with an intraperitoneal injection of 60–90 mg/kg pentobarbital.

Isolation

Cremasters were either rapidly removed and placed in 2% paraformaldehyde (PFA) for 30 minutes at room temperature for in situ experiments or were immediately placed in liquid nitrogen-cooled isopentane and transferred to OCT for sectioning. Mouse aortas were also quickly removed and placed in liquid nitrogen-cooled isopentane and transferred to OCT for sectioning. Rat mesentery (kindly provided by B. R. Wamhoff) was removed and immediately placed in 2% PFA for in situ immunocytochemistry.

Immunohistochemistry

Frozen sections were fixed with 50:50 acetone/methanol mixture for 3 minutes at −20ºC. Cx43-transfected HeLa cells (kind gifts of E. C. Beyer) were fixed with 2% PFA for 10 minutes at room temperature. In all cases, immunocytochemistry was performed as

described (5;6). In mouse cremaster, F-actin was labeled with phalloidin conjugated with Alexa594 (Invitrogen) at 1:250 for 45 mins. All immunohistochemistry samples were observed using an Olympus Fluoview confocal microscope.

Antibodies

Cx37 and Cx40 antibodies were from ADI with specificity tested as previously described for mouse (6). Two Cx43 antibodies were used, a polyclonal and a monoclonal (Sigma) (6;17). The rabbit Cx45 antibody was raised against the carboxyl terminus of mouse Cx45 and has previously been extensively tested and verified (kind gift from T. H. Steinberg, Washington University) (14). Primary antibodies against phosphorylated Cx43 at serine 368 (Cx43-S368) were obtained from Cell Signaling Technologies (1). CD31 (PECAM-1; (34)), NG2 (19), N-cadherin (Zymed (25)) and monoclonal desmin (Sigma) antibodies have all previously been tested. All primary antibodies were identified using secondary antibodies conjugated with Alexa 488 (Invitrogen).

Visualizing of proteins between EC and VSMC

Cremasters were pinned down on Sylgard-coated polyester petri-dishes and the first arteries supplied by feed arteries were identified as described (33). Once identified, the confocal microscope was activated and a 100X 1.0 N.A. water immersion lens was used to identify the EC and VSMC within the arterioles using phalloidin-Alexa594. We were unable to detect any significantly autofluorescence at the IEL (e.g., Supplementary Fig 1) in the 488 channel. XY Sections in the Z-direction at 0.2 μm steps brought a focal plane into focus containing VSMC perpendicular to the EC as determined by transverse views of VSMC which appeared as circles due to the phalloidin staining of the cortical actin and lateral cortical actin lines of the EC (Fig 1A–B and Supplementary Fig 1). The Fluoview software was used to zoom in on short segments (the end result of the zoom was approximately one to two VSMC across, or a 2X zoom). Unstained (i.e., cell-free) areas such as the IEL appeared black between the phalloidin-stained EC and VSMC, with “actin bridges” linking the two cell types (Fig 1C). The actin bridges were membrane-associated as demonstrated with staining for the fixable membrane stain FM 1–43FX (Fig 1D) indicating membranous and cytoskeletal extensions into the normally cell-free IEL. Although we can not be at all certain the actin bridges are MEJs, these observations in mouse cremaster arterioles correlate with MEJs found in mouse cremaster arterioles ((7) and personal communication, S. Sandow).

When fluorescence from an antibody was thought to be localized between EC and VSMC (Fig 2A), the fluorescence emitted from phalloidin was used to plot horizontal and vertical intensity lines to define the approximate location of an actin bridge (Fig 2B). Using the pixel intensity lines for phalloidin, a horizontal line running through the IEL would have little to no intensity unless it came across an area of fluorescence representing actin (Fig 2B, horizontal histogram), whereas a vertical intensity line would have high intensity from EC and VSMC until it came across the cell-free IEL (Fig 2B, vertical histogram). The horizontal intensity line was moved vertical until the intensity histogram was nearly flat with high intensity due to the phalloidin in EC and VSMC. The vertical intensity line was moved horizontal until the intensity histogram was nearly flat with high intensity due to the phalloidin in EC, the actin bridge, and VSMC. The intersections of the new vertical and horizontal intensity lines formed a box unique to each actin bridge. Due to irregular MEJ shapes and sizes, these intensity lines were moved 5% outward to encompass as much area as possible; this formed a region of interest (ROI) over the actin bridge unique to each particular actin bridge tested (Fig 2B, blue box).

So as to compare the relative fluorescence from the antibodies in EC, the actin bridge, and on the VSMC, the ROI box created above was placed over the fluorescent image from the

antibody being tested (Fig 2C, box 2), as well as the EC immediately above (Fig 2C, box 1) and below in the VSMC (Fig 2C, box 3). The mean pixel intensities within each of these ROI boxes were plotted on a histogram (Fig 2C). If the mean intensity within the actin bridge ROI was not within an arbitrary value of 25% of the lowest mean intensity (Fig 2C gray line; lowest mean intensity had to be 50% over background) in the EC or VSMC, the antibody was not considered "present" on the actin bridge. If the mean pixel intensity in the actin bridge ROI was at or above 25%, the protein was considered present and scored. The 25% value was chosen as we assumed that 75% of the intensity of the protein in the EC or VSMC would be similar within the MEJ. In the example from Fig 2, the probed protein of interest (Cx43) was considered present on the actin bridge. In Supplementary Fig 2, we provide an example of when the protein is not considered present on the actin bridge. The "percent positive thresholds for antibody" on the actin bridge was derived by dividing the number of actin bridges where the antibody was detected by the total number observed.

In an attempt to determine how often we were capable of detecting protein on the actin bridges, we utilized a minimum of three different animals per antibody tested. Within each of these animals, a minimum of five actin bridges were identified per arteriole. This resulted in a minimum of 15 actin bridges observed per antibody tested. Every attempt was made to randomize the choosing of actin bridges; this was done by scanning and identifying first-order arterioles that immediately came into focus and using only the actin bridge in the center most of the field of view. No other actin bridges were used for three full fields of views up or down the length of the arteriole. When examining relationships between proteins tested, significance was set at $P<0.05$ using binary population proportion statistics. This method of actin bridge and antibody reactivity determination was also applied to rat mesentery.

Results

Heterogeneous protein expression on actin bridges between EC and VSMC

Although connexin expression in mouse cremasteric arterioles can be identified in cross-section (Supplementary Fig 3), we sought to delineate connexin expression between EC and VSMC. Using actin bridges as a guide, we used the methodology described in Fig 1 to examine connexin expression. Using this technique, we observed that both Cx37 and Cx45 had variable expression patterns (Fig 3B, E), whereas both Cx40 and Cx43 were routinely found on the actin bridges (Fig 3C–D). Intensity plots under each image for both actin and connexin demonstrate apparent co-localization.

Connexin phosphorylation on actin bridges between EC and VSMC

Gap junctional coupling between EC and VSMC in mouse cremaster has recently been reported to be poor or non-existent (26). For this reason, we tested the hypothesis that the Cx43 on the actin bridges was phosphorylated at serine 368, a PKC mediated phosphorylation event that is correlated with closure of gap junctions (12). Extensive testing of the Cx43-S368 antibody demonstrated its specificity (Supplementary Fig 4 and (12)). It is well accepted that Cx43 is expressed in VSMC of the mouse aorta (27) a result we confirm (Supplementary Fig 4). In an initial test of the phosphorylated antibody, we applied it to unfixed frozen sections of mouse aorta and could only demonstrate minimal staining (Fig 4A), indicating Cx43-S368 phosphorylation did not predominate in the aortic vessel wall. In contrast to the aorta, the arterioles from mouse cremaster muscle were positive for Cx43-S368 in both the EC and VSMC (Fig 4B), as is evident in higher magnification images (Fig 4C). Actin bridges in mouse cremaster arterioles were positive for the Cx43-S368 staining (Fig 4D).

Determination of protein expression on actin bridges between EC and VSMC

Using the methods described in Fig 2, the frequency of detectable protein expression at the actin bridges is shown in Fig. 5. Neither NG2 (5.0%) nor CD31 (10.0%) were detectable at appreciable levels on actin bridges (Fig 5A). Desmin, a smooth muscle cell cytoskeletal component, and N-cadherin, an adhesion protein, were detected in 77.2%, and 70.9% respectively of the bridges sampled (Fig 5A). There was a significant difference in expression between the NG2 and CD31 antibodies and the N-cadherin and desmin antibodies (as demonstrated in raw images in Supplementary Fig 5). There was minimal expression of Cx45 (13.0%), and Cx37 expression appeared to be variable (31.8%; Fig 5A). Cx40 (83.8%) had the highest percent expression on the actin bridges, whereas Cx43 (54.2%) was also expressed (Fig 5A). Of interest is the Cx43-S368 percent staining (52.7%; Fig 5A) that was closely matched with that of Cx43 suggesting that all of the Cx43 was phosphorylated. When Cx40 was compared to any of the other connexins antibodies tested, there was a significant difference in expression. The incidence of these proteins lends increased confidence to the pattern of staining described in Fig 3.

We sought to confirm our methodology with previously published results of immunohistochemistry of connexin proteins on electron microscopy images of the MEJ (23). Both Cx37 (67.9%) and Cx40 (73.9%) were found on actin bridges, whereas Cx43 and Cx43-S368 was more variable (34.8% and 15.5% respectively; Fig 5B; as demonstrated in raw images in Supplementary Figure 6). Cx45 was rarely found on actin bridges (13.0%; Fig 5B). These results are consistent with electron microscopy images of connexin proteins previously reported for rat mesentery (23) and lend evidence to the correlation between actin bridges and MEJs.

Discussion

The technique described has allowed for determination of the incidence of protein expression between EC and VSMC. This method has the potential to be used as a screening mechanism for proteins that may be important for EC and VSMC integration. It can not however be used to determine from which cell type the protein is derived due to the multiple types of cellular extensions composing MEJs found in vivo (e.g., (20); Supplementary Fig 7). Identification of specific cell types involved will continue to require immunocytochemistry on TEM sections, or isolation of the EC and VSMC individually. Other drawbacks are discussed below.

It is clear the actin bridges are membranous (Fig 1D), which indicates that they are cellular extensions from EC, VSMC, or both. Thus, the identified proteins are at least uniquely found on cellular extensions protruding into the IEL. However, the identified proteins, using polyclonal antibodies, present a problem as it is not likely that all antibodies have the same affinity for the antigen, or indeed the same accessibility of the antibodies due to protein-protein interactions (e.g., Cx43 and N-cadherin interactions (24;31)). Another potential problem is our use of a single plane of focus, and the MEJ arguably resembles more of a cylindrical structure and we therefore believe it is a possibility that we have not correctly identified some of the protein that is expressed. In addition, we expanded the guide lines for the ROI out by 5% when analyzing protein expression on the actin bridges. This was done due to the variability in MEJ structures (20); however it is likely we have added contamination from the EC and VSMC as a whole into our analysis. Lastly, our method of collecting samples was to randomly choose actin bridges and then move three fields of view up or down the length of the arteriole. Although this technique was done in an attempt to determine relationships between different proteins being expressed on actin bridges, this actually prevented us from determining if shorter segments of the arterioles had differential expression of the connexins than other segments. Regardless of these problems, we are

encouraged by the differences demonstrated in protein expression, which implicate selective protein segregation to the actin bridges, and the correlation of this technique to previously published TEM images of connexins at the MEJ (23).

Incidence of connexin isoform within and between EC and VSMC

Using TEM, there are reports of connexin expressed at the MEJ in rat mesentery (23) and rat cerebral arteries (3). Based on the reported connexins from these studies and others (e.g., (17;27)), we selected a panel of vascular connexins to examine at actin bridges, including Cx45, Cx37, Cx40 and Cx43. When Cx45 was examined using our model, the expression on the actin bridges was consistently at low levels (Fig 5A–B). The expression of Cx45 in mouse EC and VSMC of the microcirculation has previously been demonstrated in situ using lacZ (30) and by RT-PCR in primary culture of EC.(4) There is little known about Cx45 in the microcirculation, although $Cx45^{-/-}$ mice had considerable vascular defects, indicating the importance of the particular connexin during vascular development (9).

In this study, Cx37 on actin bridges (31.8%) appeared to be variable in expression (Fig 5A), a result consistent with previous reports of Cx37 variability in mouse kidney arterioles (personal communication, N. H. Holstein-Rathlou) and the lack of a pronounced $Cx37^{-/-}$ vascular phenotype (27). It is interesting to note that murine cell culture models have also demonstrated limited or no Cx37 expression at points of heterocellular contact (6). While the in vivo data here does demonstrate minor expression of Cx37 at the MEJ, in both the culture model and in vivo Cx40 and Cx43 predominated. We can not however rule out that Cx37 may have an important role in discreet segments of the arteriole which may have accounted for the variability observed. Although, in rat mesentery there was no detectable variability of Cx37 expression at the point of heterocellular contact (e.g., compare Fig 5A and Fig 5B, as well as (23)). It is clear more work is required to understand these observations.

In our studies, Cx40 was the most consistent connexin tested to be found on actin bridges in mouse cremaster (Fig 5A). Because this connexin is found in EC and not VSMC (27) it is likely that this connexin is selectively placed on the EC side of the MEJ which corresponds with reports of Cx40 at the MEJ in rat (23). It is unclear how exactly Cx40 in mouse cremaster muscle integrates EC and VSMC, but previous experiments have demonstrated that Cx40 antibody could block endothelium-derived hyperpolarizing factor (EDHF) in rat mesentery (18).

Recently Cx43 was identified as being important in the transmission of EDHF in humans (13), a result that coincides with our report of Cx43 on actin bridges in the majority of experiments (Fig 5A). Because Cx43 was expressed in both EC and VSMC (Supplementary Fig 3), it was unclear whether both cell types contributed the connexins on the actin bridge. It is not clear why Cx43 was expressed over 50% of the time on actin bridges, but not as often as Cx40.

There is a difference in phosphorylation states in rat Cx43 as compared to mouse Cx43 (Fig 5A to Fig 5B). In the mouse, the Cx43 present on the actin bridges is almost always phosphorylated by Cx43-S368, however, little Cx43 was detected on actin bridges in rat, and it was rarely found to be phosphorylated at serine 368. The Cx43 phosphorylation event at the MEJ may be a rationale for why EDHF responses are routinely noted in rat mesentery, but not in mouse cremaster (26) (see below).

Connexin phosphorylation on actin bridges

Gap junctions are not passive holes between cells, but are highly regulated in terms of opening, closing and solute movement. The regulation of the gap junction can be on time

scales relating to connexin turnover (approximately one to four hours), or on time scales that are much shorter. The factors that can quickly regulate gap junction permeability include intracellular pH and Ca^{2+} concentrations (21), as well as nitrosylation (8) and phosphorylation (10). Each of these factors has been shown to be able to occur in discreet domains within cells, making it possible that regulation of gap junctions could occur within localized cellular areas, e.g., the MEJ.

In the present study, we examined whether connexin phosphorylation was present on the actin bridges in mouse cremaster. The rationale for this arose from the knowledge that, anatomically, gap junctions are present at the MEJ (e.g., (6;22;29)); however, functional evidence in mouse cremaster has disputed their role at the MEJ (26). The descriptive evidence presented herein demonstrates that Cx43 is phosphorylated at S368. Phosphorylation of this site is generally considered to "close" gap junction based communication (11;12;28), although it is not clear what effect, if any, there is on any other connexin proteins (i.e., they could still remain "open"). We can not exclude the possibility that factors inherit to the cremasteric removal (e.g., tissue damage and release of ATP) could also be the cause of the phosphorylation event. Taken together, we hypothesize that connexin phosphorylation observed on actin bridges in mouse cremaster may be the reason that poor EC-VSMC coupling has previously been reported. Future experiments that *directly* test the effects of connexin phosphorylation at the MEJ and their functional consequences will be required.

Conclusion

In summary, we have demonstrated a method utilizing actin bridges between EC and VSMC to localize proteins at the interface between the two cell types. The incidence of the protein found on the actin bridges was dependant on the connexin isoform and the correlation with this method and TEM images of connexin expression at the MEJ in rat mesenteric arteries implicate that the actin bridges were possibly MEJs. We therefore believe that this method is an important first-step towards actual quantification of protein found between EC and VSMC, possibly at MEJs.

Supplementary Material

Refer to Web version on PubMed Central for supplementary material.

Acknowledgments

The authors thank with appreciation expertly performed initial experiments performed by Kathy Day and David Damon. Critical comments on the manuscript were provided by Dr. Robin Looft-Wilson and Michael Rizzo. Histological preparations were performed by the University of Virginia Research Histology Lab. The work was supported by an American Heart Association Beginning Grant-in-Aid (BEI), American Heart Association Science Development Grant (BEI), the Robert M. Berne Cardiovascular Research Center Partner's Fund (BEI), NIH HL088554 (BEI) and NIH HL53318 (BRD).

Reference List

1. Ek-Vitorin JF, King TJ, Heyman NS, Lampe PD, Burt JM. Selectivity of connexin 43 channels is regulated through protein kinase C-dependent phosphorylation. Circ Res 2006;98:1498–1505. [PubMed: 16709897]
2. Elfgang C, Eckert R, Lichtenberg-Frate H, Butterweck A, Traub O, Klein RA, Hulser DF, Willecke K. Specific permeability and selective formation of gap junction channels in connexin-transfected HeLa cells. J Cell Biol 1995;129:805–817. [PubMed: 7537274]
3. Haddock RE, Grayson TH, Brackenbury TD, Meaney KR, Neylon CB, Sandow SL, Hill CE. Endothelial coordination of cerebral vasomotion via myoendothelial gap junctions containing

connexins 37 and 40. Am J Physiol Heart Circ Physiol 2006;291:H2047–H2056. [PubMed: 16815985]

4. Hirschi KK, Burt JM, Hirschi KD, Dai C. Gap junction communication mediates transforming growth factor-beta activation and endothelial-induced mural cell differentiation. Circ Res 2003;93:429–437. [PubMed: 12919949]
5. Isakson BE, Damon DN, Day KH, Liao Y, Duling BR. Connexin40 and connexin43 in mouse aortic endothelium: evidence for coordinated regulation. Am J Physiol Heart Circ Physiol 2006;290:H1199–H1205. [PubMed: 16284228]
6. Isakson BE, Duling BR. Heterocellular contact at the myoendothelial junction influences gap junction organization. Circ Res 2005;97:44–51. [PubMed: 15961721]
7. Isakson BE, Ramos SI, Duling BR. Ca2+ and inositol 1,4,5-trisphosphate-mediated signaling across the myoendothelial junction. Circ Res 2007;100:246–254. [PubMed: 17218602]
8. Kameritsch P, Khandoga N, Nagel W, Hundhausen C, Lidington D, Pohl U. Nitric oxide specifically reduces the permeability of Cx37-containing gap junctions to small molecules. J Cell Physiol 2005;203:233–242. [PubMed: 15481066]
9. Kruger O, Plum A, Kim JS, Winterhager E, Maxeiner S, Hallas G, Kirchhoff S, Traub O, Lamers WH, Willecke K. Defective vascular development in connexin 45-deficient mice. Development 2000;127:4179–4193. [PubMed: 10976050]
10. Lampe PD, Lau AF. Regulation of gap junctions by phosphorylation of connexins. Arch Biochem Biophys 2000;384:205–215. [PubMed: 11368307]
11. Lampe PD, Lau AF. The effects of connexin phosphorylation on gap junctional communication. Int J Biochem Cell Biol 2004;36:1171–1186. [PubMed: 15109565]
12. Lampe PD, TenBroek EM, Burt JM, Kurata WE, Johnson RG, Lau AF. Phosphorylation of connexin43 on serine368 by protein kinase C regulates gap junctional communication. J Cell Biol 2000;149:1503–1512. [PubMed: 10871288]
13. Lang NN, Luksha L, Newby DE, Kublickiene K. Connexin 43 mediates endothelium-derived hyperpolarizing factor-induced vasodilatation in subcutaneous resistance arteries from healthy pregnant women. Am J Physiol Heart Circ Physiol 2007;292:H1026–H1032. [PubMed: 17085540]
14. Lecanda F, Towler DA, Ziambaras K, Cheng SL, Koval M, Steinberg TH, Civitelli R. Gap junctional communication modulates gene expression in osteoblastic cells. Mol Biol Cell 1998;9:2249–2258. [PubMed: 9693379]
15. Little TL, Beyer EC, Duling BR. Connexin 43 and connexin 40 gap junctional proteins are present in arteriolar smooth muscle and endothelium in vivo. Am J Physiol 1995;268:H729–H739. [PubMed: 7864199]
16. Locke D, Stein T, Davies C, Morris J, Harris AL, Evans WH, Monaghan P, Gusterson B. Altered permeability and modulatory character of connexin channels during mammary gland development. Exp Cell Res 2004;298:643–660. [PubMed: 15265710]
17. Looft-Wilson RC, Payne GW, Segal SS. Connexin expression and conducted vasodilation along arteriolar endothelium in mouse skeletal muscle. J Appl Physiol 2004;97:1152–1158. [PubMed: 15169746]
18. Mather S, Dora KA, Sandow SL, Winter P, Garland CJ. Rapid endothelial cell-selective loading of connexin 40 antibody blocks endothelium-derived hyperpolarizing factor dilation in rat small mesenteric arteries. Circ Res 2005;97:399–407. [PubMed: 16037574]
19. Murfee WL, Skalak TC, Peirce SM. Differential arterial/venous expression of NG2 proteoglycan in perivascular cells along microvessels: identifying a venule-specific phenotype. Microcirculation 2005;12:151–160. [PubMed: 15824037]
20. Rhodin JA. The ultrastructure of mammalian arterioles and precapillary sphincters. J Ultrastruct Res 1967;18:181–223. [PubMed: 5337871]
21. Saez JC, Berthoud VM, Branes MC, Martinez AD, Beyer EC. Plasma membrane channels formed by connexins: their regulation and functions. Physiol Rev 2003;83:1359–1400. [PubMed: 14506308]
22. Sandow SL, Hill CE. Incidence of myoendothelial gap junctions in the proximal and distal mesenteric arteries of the rat is suggestive of a role in endothelium-derived hyperpolarizing factor-mediated responses. Circ Res 2000;86:341–346. [PubMed: 10679487]

23. Sandow SL, Neylon CB, Chen MX, Garland CJ. Spatial separation of endothelial small- and intermediate-conductance calcium-activated potassium channels (K(Ca)) and connexins: possible relationship to vasodilator function? J Anat 2006;209:689–698. [PubMed: 17062025]
24. Shaw RM, Fay AJ, Puthenveedu MA, von Zastro M, Jan YN, Jan LY. Microtubule plus-end-tracking proteins target gap junctions directly from the cell interior to adherens junctions. Cell 2007;128:547–560. [PubMed: 17289573]
25. Shoval I, Ludwig A, Kalcheim C. Antagonistic roles of full-length N-cadherin and its soluble BMP cleavage product in neural crest delamination. Development 2007;134:491–501. [PubMed: 17185320]
26. Siegl D, Koeppen M, Wolfle SE, Pohl U, de Wit C. Myoendothelial coupling is not prominent in arterioles within the mouse cremaster microcirculation in vivo. Circ Res 2005;97:781–788. [PubMed: 16166558]
27. Simon AM, McWhorter AR. Vascular abnormalities in mice lacking the endothelial gap junction proteins connexin37 and connexin40. Developmental Biology 2002;251:206–220. [PubMed: 12435353]
28. Solan JL, Fry MD, TenBroek EM, Lampe PD. Connexin43 phosphorylation at S368 is acute during S and G2/M and in response to protein kinase C activation. J Cell Sci 2003;116:2203–2211. [PubMed: 12697837]
29. Taugner R, Kirchheim H, Forssmann WG. Myoendothelial contacts in glomerular arterioles and in renal interlobular arteries of rat, mouse and Tupaia belangeri. Cell Tissue Res 1984;235:319–325. [PubMed: 6705035]
30. Theis M, Mas C, Doring B, Degen J, Brink C, Caille D, Charollais A, Kruger O, Plum A, Nepote V, Herrera P, Meda P, Willecke K. Replacement by a lacZ reporter gene assigns mouse connexin36, 45 and 43 to distinct cell types in pancreatic islets. Exp Cell Res 2004;294:18–29. [PubMed: 14980497]
31. Wei CJ, Francis R, Xu X, Lo CW. Connexin43 associated with an N-cadherin-containing multiprotein complex is required for gap junction formation in NIH3T3 cells. J Biol Chem 2005;280:19925–19936. [PubMed: 15741167]
32. Wei CJ, Xu X, Lo CW. Connexins and cell signaling in development and disease. Annu Rev Cell Dev Biol 2004;20:811–838. [PubMed: 15473861]
33. Wiedeman MP. Blood flow through terminal arterial vessels after denervation of the bat wing. Circ Res 1968;22:83–89. [PubMed: 5635209]
34. Wu X, Rabkin-Aikawa E, Guleserian KJ, Perry TE, Masuda Y, Sutherland FW, Schoen FJ, Mayer JE Jr, Bischoff J. Tissue-engineered microvessels on three-dimensional biodegradable scaffolds using human endothelial progenitor cells. Am J Physiol Heart Circ Physiol 2004;287:H480–H487. [PubMed: 15277191]

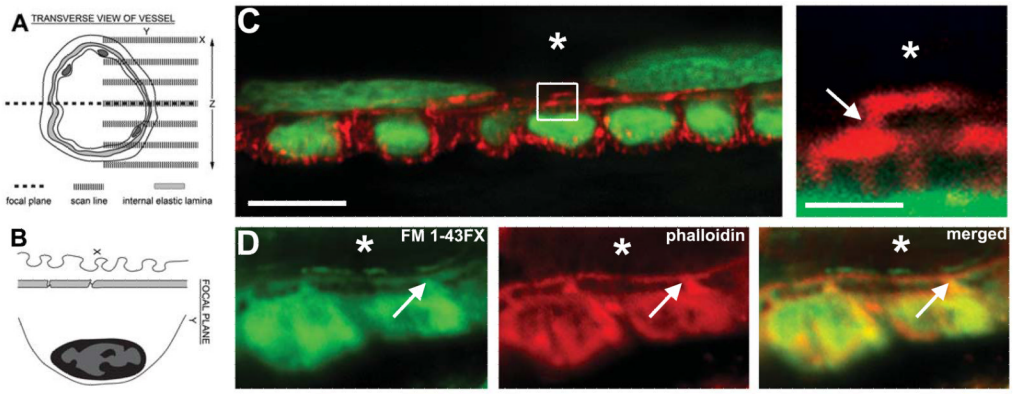

Figure 1. Actin-based structures between endothelium and vascular smooth muscle within mouse cremaster arterioles

A, multiple XY images were sectioned in the Z direction through an intact arteriole until a transverse image was resolved (dotted line), as demonstrated by the orientation in B. The image in C demonstrates a transverse image of an arteriole stained for phalloidin (red) and the nuclear marker SYTOX (green). Orientation of nuclei demonstrates endothelium (top) perpendicular to smooth muscle (bottom). The box in C is enlarged on right. In D, the phalloidin (red) and the FM 1–43FX (green) appear in the same location between EC and SMC. Bars in C are 10 μm (left) and 2 μm (right) and in D, bar is 5 μm. Asterisks indicate lumen, arrows indicate actin bridges.

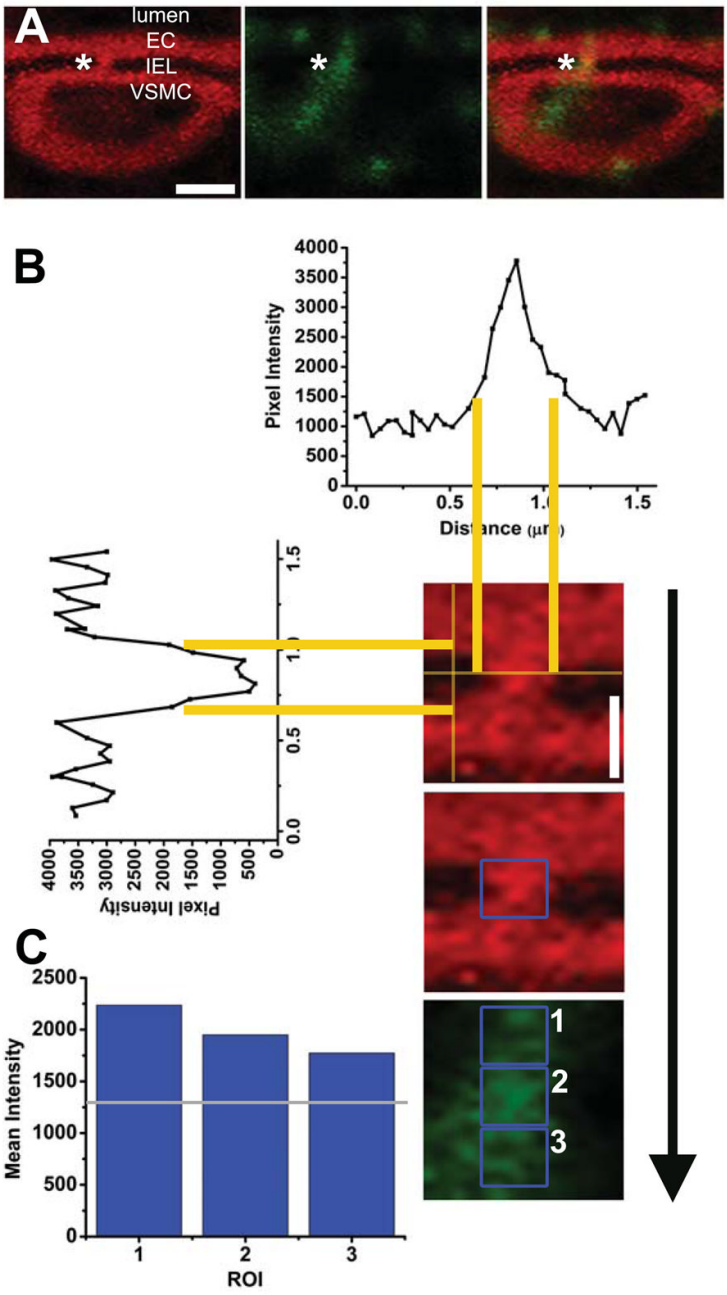

Figure 2. Methodology for determination of the incidence of protein expression on actin bridges

A, arteriole double stained with phalloidin (red) and Cx43 (green); asterisks indicating the actin bridge between VSMC and EC. In B, representative intensity plots running horizontal and vertical defined the IEL and approximate localization of an actin bridge indicated by asterisk in A. Yellow lines are guides for localization of intensity on the histograms. The intersections of the new vertical and horizontal intensity lines formed a box unique to each actin bridge. Due to irregular MEJ shapes and sizes, these intensity lines were moved 5% outward to encompass as much area as possible; this formed a ROI over the actin bridge (blue box). In C, blue boxes demonstrate the ROI for EC (1), the actin bridge (2), and VSMC (3). The mean pixel intensity from each of these boxes is in histogram format in C. The grey line is 25% below the value in ROI 3 and used as a bench mark for pixel intensity

in ROI 2. In this incidence, the protein is found on the actin bridge. See Materials and Methods for details. White bar in A is 3 μm and is representative for all other images in A; in B, white bar is 1 μm and is representative for all other images in B and C.

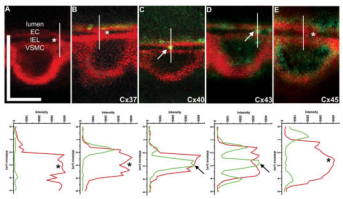

Figure 3. Connexin expression on the actin bridges

A, in control conditions with phalloidin (red) and secondary antibody alone, there is no apparent staining at the actin bridges. In B, there is no Cx37 (green) evident on the actin bridge. C, Staining for Cx40 (green) is found on the actin bridge. D, Cx43 (green) is also found on the actin bridge and in E, Cx45 (green) expression is not found on the actin bridges. Vertical white lines running through the actin bridges correspond to the intensity plots below each image. In these plots, the intensity of the fluorescence in red (actin) and green (connexin) are plotted against the distance (in μm). Asterisks indicate unstained actin bridges whereas arrows demonstrate protein expression on the actin bridges. In A, vertical bar is 10 μm and horizontal bar is 5 μm and is representative for all images.

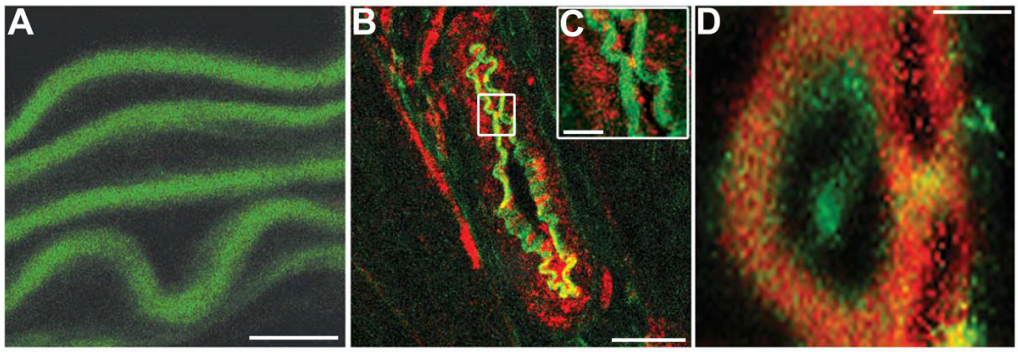

Figure 4. Cx43-S368 phosphorylation on the actin bridges

In A–C, green is IEL, red is Cx43-S368. A, there is no Cx43-S368 detectable in the aorta. However, in B–C, transverse sections of mouse cremasteric arterioles demonstrate heavy staining for Cx43-S368 in EC and VSMC. C, is an enlarged image from B (white box). D, actin bridges are highlighted by phalloidin (red); Cx43-S368 (green) is clearly seen between cell types. Bar in A is 40 μm, bar in B is 20 μm; bar in C is 10 μm; and bar in D is 5 μm.

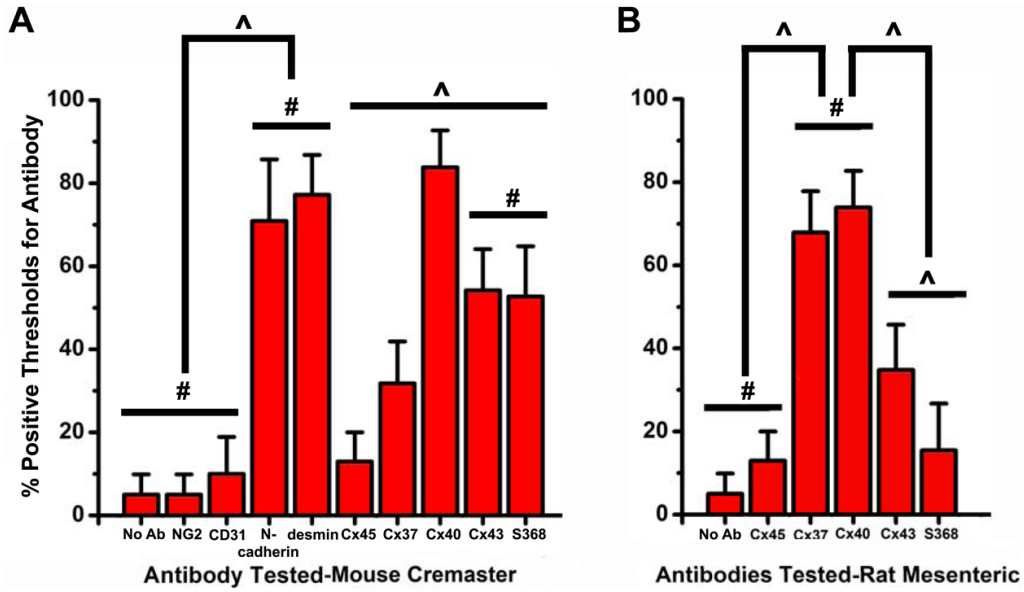

Figure 5. Determination of antibody threshold detection on the actin bridges

Using the methods described in Materials and Methods and in Fig 2, histograms of percent of time that a proteins could be detected on an actin bridge was plotted in A, mouse cremaster arterioles and B, rat mesenteric arteries. Bars are standard deviation. The symbol "#" represents no significant difference; "^" represents a significant difference.